Solid Phase Microextraction-Multi Capillary Column-Ion Mobility Spectrometry (SPME-MCC-IMS) for Detection of Methyl Salicylate in Tomato Leaves

Vahideh Ilbeigi[1], Younes Valadbeigi[2,3], Ľudmila Slováková[4] and Štefan Matejčík[1]

[1]Department of Experimental Physics, Comenius University, Mlynská dolina F2, 84248 Bratislava, Slovakia

[2] Department of Chemistry, Faculty of Science, Imam Khomeini International University, Qazvin, Iran.

[3] University of Natural Resources and Life Sciences, Department of Chemistry, Institute of Analytical Chemistry, 1190 Vienna, Austria

[4] Department of Plant Physiology, Faculty of Natural Sciences, Mlynská dolina, Ilkovičova 6, 842 15 Bratislava 4, Slovakia

Emails: vahideh.ilbeigi@fmph.uniba.sk; stefan.matejcik@fmph.uniba.sk

Abstract

Methyl salicylate (MeSA) is a plant-signaling molecule that plays an essential role in the regulation of the plant responses to biotic and abiotic pathogens. In this work, solid phase microextraction (SPME) and multi-capillary column (MCC) are coupled to ion mobility spectrometer (IMS) to detect MeSA in tomato leaves. The SPME-MCC-IMS method provides two-dimensional (2D) separation by both MCC and IMS, based on the retention and drift times. The effect of the IMS polarity on the separation efficiency of MCCs was also investigated. In the positive polarity, ionization of MeSA resulted in ($[MeSA+H]^+$) while in the negative deprotonated ions ($[MeSA-H]^-$) and O_2^- adduct ion ($[MeSA+O_2]^-$ were formed. In the real sample analysis, the negative polarity operation resulted in the suppression of many matrix molecules and thus in the reduction of interferences. Four different SPME fibers were used for head space analysis and four MCC columns were investigated. In the negative polarity, complete separation was achieved for all the MCCs columns. The limits of detection (LODs) of 15 and 22 ppb (v/v) were achieved for the direct injection of head space of MeSA in positive and negative polarities, indicating high sensitivity of IMS toward MeSA. Limits of detection (LOD) of 0.1 µg g^{-1} and linear range of 0.25-14 µg g^{-1} were obtained for measurement of MeSA by the SPME-MCC-IMS method with 5 min extraction time. The MeSA content of fresh tomato leaves were determined as 1.5-9.8 µg g^{-1}, 24-96 h after inoculation by tomato mosaic virus (ToRSV).

1. Introduction

Plant hormones (PHs) or phytohormones, are signaling molecules produced within plants influencing the plant growth, seed germination, fruit maturation and fruit ripening and control the physiological processes including the embryogenesis, regulation of the organ size, pathogen defense, and reproductive developments.[1,2] Hence, the quantitative analysis of the PHs and determination of their concentrations in different tissues is crucially important to understand the role of these molecules in physiological processes occurring in plants. Classical biological methods such as bioassay and immunoassay were the first methods employed for quantification of the PHs. However, these methods suffer from low precision because of interfering effects of other compounds, which resulted in the problems related to linearity, sensitivity and reproducibility of response.[3-5]

Because of the complex matrix of the plant extracts and the low concentration of the PHs in the plant tissues, the methods for analysis of PHs require extraction, pre-concentration, and analytical techniques with high sensitivity. The solid phase (micro)extraction (SPME) with different modified surfaces and compositions is widely used for the purification, pre-concentration, and extraction of the PHs.[6-11] To date, several analytical methods have been developed for sensitive quantitative and qualitative analysis of PHs in different parts of fruits and plants using chromatographic techniques, mainly liquid chromatography (LC) and gas chromatography (GC), in combination with mass spectrometry (MS). GC-MS and LC-MS can be used for simultaneous analysis of PHs mixtures and provide a wide linear dynamic range (≥ 2 order) and limit of detection (LOD) less than few μg g^{-1}.[12-17] There are also other methods based on techniques such as capillary electrophoresis,[18,19] Raman spectroscopy,[20,21] and desorption electrospray ionization mass spectrometry imaging.[22]

Methyl salicylate (MeSA), synthesized in plants from salicylic acid (SA), is a plant hormone which plays an important role in the resistance of plants to pathogens, thermogenesis in some flowers, and flower durability.[1,2,23] Numerous methods have been developed for determination of MeSA in leaves and fruits of plants and its vapor in gas phase.[24-28] The reported amounts of MeSA in tomato and white tea leaves are in the range of 1-7 μg g^{-1}.[29-31] Concentration of MeSA in the tomato leaves change with time after inoculation with a pathogen, however, the change is within the above range.[29]

The above-mentioned methods involve costly apparatus and require a high degree of technical knowledge. Ion mobility spectrometry (IMS) is a fast, inexpensive, and sensitive technique with growing application in analysis of various classes of analytes.[32-36] In IMS, the analytes are vaporized and ionized in an ion source, then, the produced ions move toward a detector under an electric field through a drift gas (mainly air, or N_2). The ion separation is based on

the interactions of ions with the buffer gas under action of an electric field (depends on the drift gas, m/z, geometry of ions, pressure, and temperature).[37] IMS can be operated in both positive and negative polarities for detection of cations and anions, respectively. Over the past few years, SPME coupled to IMS has been used for collection and preconcentration of analytes in both gas phase and from solution for analysis by IMS.[38-39] MCCs consist of packs of parallel capillaries with inner surface covered by film of a stationary phase enables fast separation in gas phase analysis. The multi-capillary column (MCC), as a fast separation technique, in combination with IMS has found application mainly in the field of breath analysis.[40]

In this work, an IMS-based method was developed to exploit the advantages of SMPE, MCC and IMS for fast and sensitive analysis of real samples in complex matrix. The SPME-MCC-IMS method was employed for quantitative analysis of MeSA in tomato leaves.

2. Experimental Section

2.1 Materials and Methods

Methanol (99.9%) and MeSA (99%) were purchased from Sigma Aldrich. The standard samples of MeSA were prepared in a mixture of water and methanol (50:50). For direct injection measurements, 1 µL of the standard solutions was injected to the injection port using a 10 µL Hamilton syringe. A similar method as reported in ref.[30] was used to treat the tomato leaves by tomato ringspot virus (ToRSV) and prepare the leaf samples. The ToRSV inoculation buffer was obtained from Institute of Virology, Biomedical Research Center of Slovak Academy of Sciences (store at -20 ^{o}C).[41] The lower leaves of the tomato plants with an age of 5 weeks were inoculated by ToRSV. 100 mg fresh tomato leaves were taken and frozen in liquid nitrogen, ground to fine powder. Then, the sample was transferred to a 20-mL amber vial for headspace SPME analysis. The spiked samples were obtained by adding 100 µL of standard solutions (1-20 µg mL^{-1}) to 100 mg ground leaf.

The SPME fibers used in this work were commercially available SPME Arrow (Restek PAL, Switzerland) coated with (i) carbon WR/PDMS, (ii) DVB/carbon WR/PDMS, (iii) PDMS, and (iv) DVB/PDMS. Detailed description of the fiber composition of the SPME arrows is provided in Table S1 (Supporting Information). Pre and re-conditioning of the Arrow fibers were done thermally in the injection port of IMS according to the manufacturer's instruction. In the SPME experiments, the fiber was exposed to head space of 100 µL (standard solution) or 100 mg ground leaves (real sample) in a 20-mL sealed vial (Figure 1). To desorb the adsorbed compounds, the SPME fiber was put in an injection port with temperature of 220 °C. The desorbed compounds were transferred to the MCC by a carrier gas with flow rate of 50 mL min^{-1}.

Four multicapillary columns (MCCs) including OV1, OV5, OV17, OV20 (Multichrom Ltd. Russia) of 20 cm length were used for pre-separation of the volatile compounds released from tomato leaves. The stationary phases for the MCCs were as OV1: 100% - polydimethylsiloxane (non-polar), OV5: 5% - diphenyl, 95% - dimethylpolysiloxane (non-polar), OV17: 50% - diphenyl, 50% - dimethylpolysiloxane (weak-polar), and OV20: 20% - diphenyl, 80% - dimethylpolysiloxane (weak-polar). A temperature-controlled chamber was designed and constructed to house the MCC capillaries. The MCC was heated by heating elements powered by a power supply with voltage of 30 V. The temperature of MMC was kept constant during the measurements at 100±1 °C. The MCC was put between an injection port and the inlet of IMS (Figure 1). The desorbed compounds from the SPME fiber are separated in MCC before entering to the ionization region of IMS.

2. 2 Instrumentation

A standalone IMS and IMS combined with time-of-flight mass spectrometer (IMS-TOFMS)used in this study were equipped with a point to plane CD-APCI ionization source operating in both positive and negative polarities. Both IMS and IMS-TOFMS are homemade instruments constructed at the Department of Experimental Physics of Comenius University in Slovakia. A detailed description of the instruments can be found elsewhere.[39] The internal pressure and temperature of the IMS drift tube were 700 mbar and 110 ± 2 °C, respectively. A Faraday plate was used as the IMS detector at the end of the drift tube. The flow rate of the drift gas (zero air) was 700 $mLmin^{-1}$. A voltage of 8 kV was applied to the whole drift tube of IMS (12.5 cm) to provide a drift field of 640 Vcm^{-1}. The potential difference between the needle and plane electrodes of the CD ion source was 3 kV. The length of TOF–MS tube was 54.7 cm with internal pressure of 10^{-6} mbar. A multichannel plate (MCP) was used as a detector for TOF–MS.

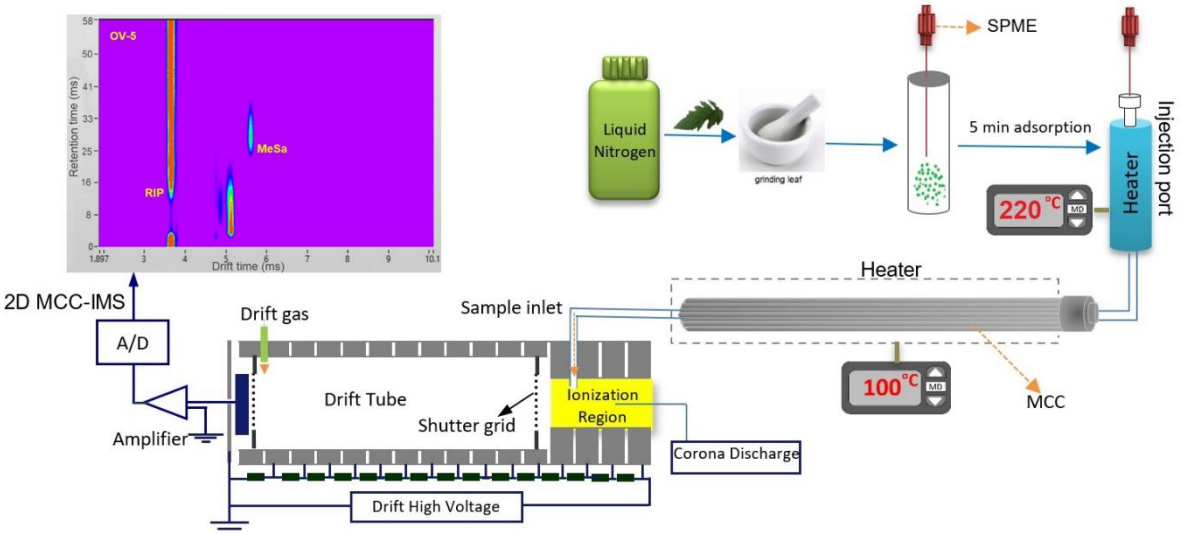

131

132 **Figure 1**. Schematic presentation of the experimental set-up.

133

134 **2.2 Computational details**

135 The structures of neutral molecules and ions were fully optimized by density functional (DFT)
136 calculations at the ωB97xD/6-311++G(d,p) level of theory. Frequency calculations were
137 carried out at 25 °C at the same level of theory to compute thermodynamic quantities including
138 enthalpies (ΔH) and Gibbs free energies (ΔG) of ion formation in the gas phase. Gaussian 16
139 software was used for all calculations.[42]

140

141 # 3. Results and Discussion

142 **3-1 Ionization mechanism of MeSA**

143 MeSA is a volatile compound with a relative high vapor pressure (0.0343 mmHg), the direct
144 injection of its head space vapor into IMS leads to signal saturation. Hence, the MeSA vapor
145 was diluted by zero air via a T-shaped connector before entering to the ionization region
146 (Supporting information, Figure S1-a). Figure 2a are compared the IMS-spectra of 100-fold
147 diluted vapor head space of MeSA in the positive and negative polarities of IMS. The
148 corresponding MS spectra in Figure 2b show that the reactant ions (RI) in the positive mode
149 are hydronium ions, $H^+(H_2O)_{3,4}$, and RIs in the negative modes are mainly O_2^- clusters with
150 H_2O and CO_2. MeSA is ionized in the positive mode via proton transfer resulting in formation
151 of $[MeSA+H]^+$ (*m/z* 153). According to the calculation of relative energies, the C=O group is
152 the preferred site of protonation in the gas phase (Supporting Information, Figure S2). In the
153 negative polarity, ionization of MeSA is resulting in two ions, deprotonated $[MeSA-H]^-$ (m/z
154 151), and adduct ion $[MeSA+O_2]^-$ (m/z 184). According to calculations, deprotonation occurs

at the phenolic OH group of MeSA. The calculations indicate that both negative ions $[MeSA+O_2]^-$and $[MeSA-H]^-$, are thermodynamically possible (Table S2), however, O_2^- adduct ion (ΔG=-129 kJ mol^{-1}) is more favorable than deprotonated ion (ΔG=-20 kJ mol^{-1}). These thermodynamics values are in accordance with the relative intensities of the $[MeSA+O_2]^-$ and $[MeSA-H]^-$ in MS.

The effect of NH_3 dopant on the ionization of MeSA in positive polarity was investigated. It was found that presence of NH_3 decreases the intensity of MeSA peak (Supporting information, Figure S3). It may be due to higher proton affinity of NH_3 compared to H_2O so that protonation of MeSA by H_3O^+ is more efficient compare to NH_4^+.

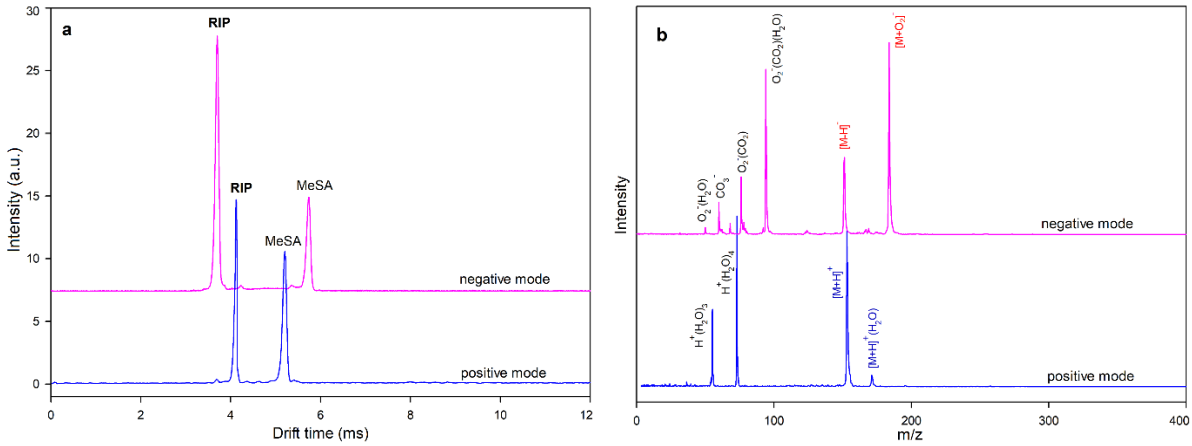

Figure 2. (a) Comparison of the (a) IMS and (b) MS spectra of MeSA in the positive and negative polarities for direct injection of 100-fold diluted vapor head space of MeSA. RIP: reactant ion peak.

3-2 Optimization of SPME sampling

The MeSA content of tomato leaves is about 1-7 µg g^{-1},[29] these concentration range was used for SPME sampling optimization. Four SMPE needles with different fiber composition were considered. The fibers were exposed to the head space of MeSA sample solution with concentration of 2 µg mL^{-1} for 30 min. Figure 3a shows a comparison of the signal intensity of MeSA for the four different SMPE fibers. Although all fibers can adsorb MeSA successfully, the maximum signal intensity was achieved for the SPME needle with PMDS fiber.

To find the optimal condition for SPME sampling, the effects of concentration, extraction time, and temperature were investigated. Figure 3b shows the effect of SPME extraction time on the signal intensity for standard samples with concentrations of 2 and 7 µg mL^{-1}. For the lower concentration 2 µg mL^{-1}, the maximum signal intensity is achieved at 30 min without any signal saturation. After 30 min, a decrease in the signal intensity was observed which was attributed to liquification of the solvent on the SPME fiber washing the absorbed MeSA. For the sample

with concentration of 7 µg mL^{-1} the signal was saturated after 10 min. Hence, 5 min was selected as an optimal extraction time of SPME to avoid saturation in the real sample measurements.

Figure S4 (Supporting information) shows the signal intensity of MeSA versus different extraction temperature for 2 µg mL^{-1} standard sample of MeSA and grounded leaves spiked with 0.2 µg MeSA with 30 min extraction time. With the increasing extraction temperature, signal intensity for the standard sample decreases. This may be due to vaporization of solvent and its liquification on the SPME fiber. However, for grounded leaves, the MeSA signal smoothly increases up to 55 °C, then the signal decreases. As the increase in the signal intensity from 25 °C to 55 °C in not significant, room temperature was used for the SPME experiments.

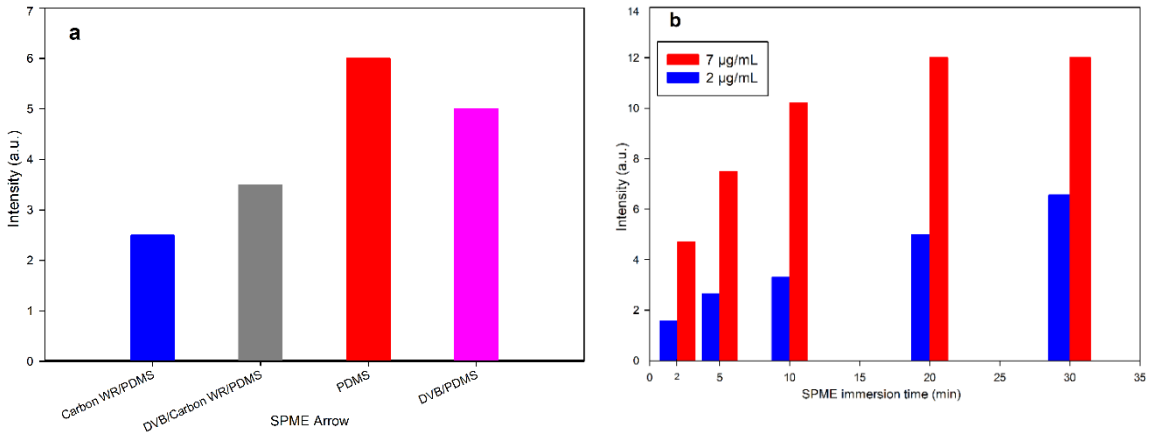

Figure 3. (a) Comparison of the signal intensity of MeSA for four SMPE needles with different fiber composition for extraction time of 30 min and MeSA concentration of 2 µg mL^{-1} in 100 µL solution (b) Effect of concentration of SPME exposure time on the signal intensity and signal saturation of SPME.

3-3 Measurement of MeSA vapor in the gas phase

MeSA is a volatile compound and its measurement in the gas phase is of interest for different purposes.[27] The limits of detection (LODs) of MeSA in the gas phase were obtained by direct infusion and by SPME preconcentration. In the case of direct infusion, the dilution was carried out by zero air with a T-shaped connector as shown in Figure S1-a (Supporting information). The calibration curves are shown in Figures S1-b and c. The obtained LODs for the direct infusion of gaseous MeSA were 15 and 22 ppb (v/v) in positive and negative polarities. Using SMPE preconcentration, LODs of 0.08 and 0.1 ppb (v/v) were achieved in positive and negative polarities. These LODs are lower than those reported for bi-enzyme electrochemical sensor (1.8 ppb)[43] and photonic crystal nanobeam cavity (1.5 ppb).[44]

3-4 Detection of MeSA in tomato leaves by SMPE-IMS and SPME-MCC-IMS methods

The goal of this study was detection of MeSA in the tomato leaves. For this purpose, the calibration curves, LODs, and linear ranges of MeSA detection in tomato leaves were obtained, using head space SPME analysis. Two types of samples were measured: (i) 100 µL of MeSA solution (0.1-20 µg ml^{-1}) as standard sample, and (ii) 100 mg grounded leaves with and without spiked MeSA. It should be mentioned that in case of direct infusion of head space of 100 mg grounded leaves spiked with 1 µg MeSA into IMS (at sampling flow rate of 10 mL min^{-1}) an IMS spectrum with few peaks of the matrix molecules, however, without MeSA peak, was observed (Supporting information, Figure S5). This could be due to low concentration of MeSA in the head space of the tomato leaves or/and suppression of the MeSA signal by the interfering molecules (preventing MeSA ionization). To avoid the interferences, pre-concentration and pre-separation by SPME and MCC were used for identification of MeSA in tomato leaves.

Using the head space SPME method with IMS, the LODs of 0.1 µg mL^{-1} were obtained for standard samples of MeSA in the negative mode with 5 min extraction times at room temperature (see Figure S6-a, Supporting information, for the calibration curve). SPME-IMS was also used for detection of MeSA in a head space a 100 mg ground leaves (Supporting information, Figure S6-b). Figure 4 compares the SPME-IMS spectra for 5 min extraction time of 100 mg ground leaves spiked with 1 µg MeSA in positive and negative modes. In the negative mode, a simpler IMS spectrum containing fewer peaks is observed. However, only a weak peak of MeSA appeared. In the positive mode, IMS spectrum shows a complicated pattern without any peak for MeSA or a small peak due to partial peak overlapping. These different behaviors are due to different ionization mechanisms in the positive and negative polarities and their efficiency for ionization of the matrix and interfering molecules. In the positive mode, ionization is mainly based on the proton transfer. Since most of organic compounds in plants have sufficient proton affinity, they can be easily ionized (protonated) in the positive polarity. In the negative polarity, only the acidic compounds are mostly ionized. In other words, ionization in the negative polarity can be considered as a more selective ionization and a less matrix molecules are ionized, resulting in IMS spectra with less interfering peaks. Although in the negative polarity only one peak of matrix molecules is observed, it suppresses the ionization of MeSA causing weak response for MeSA.

The experiments were repeated with a SPME-MCC-IMS (OV5 column) in both positive and negative polarities. The Figure 4 displays IMS spectra obtained with SPEM-IMS and SPME-MCC-IMS. In case of SPME-MCC-IMS, many additional IMS peaks appear at different

retention times of MCC, including MeSA. This indicates the importance of MCC separation for MeSA measurement in leaf tissue with IMS.

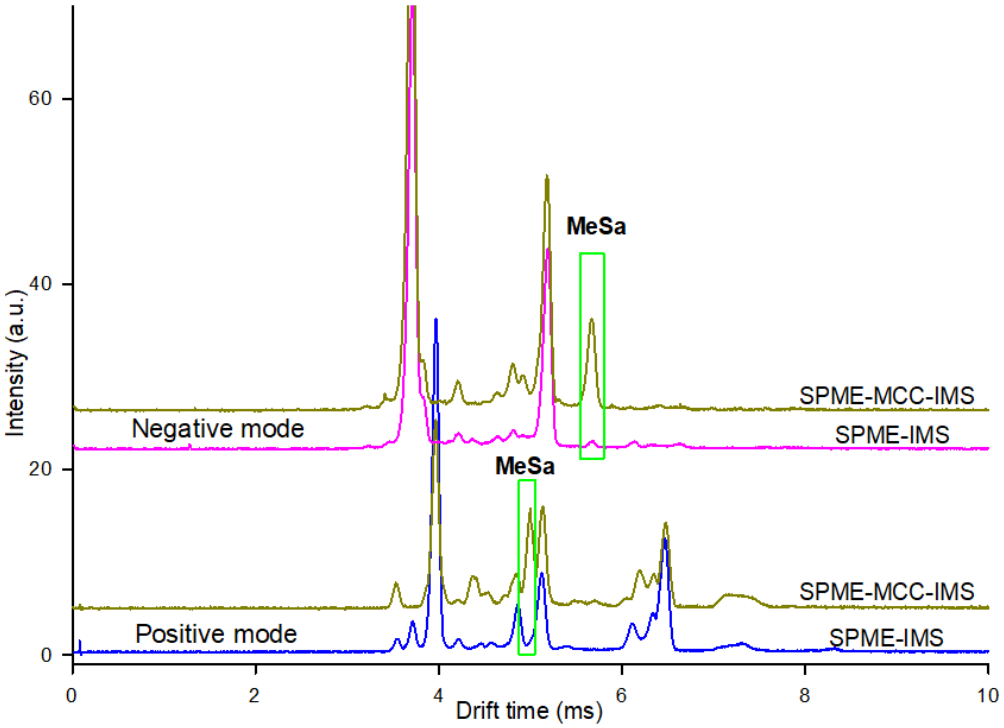

Figure 4. Comparison of the SPME-IMS and SPME-MCC-IMS spectra for 5 min extraction time of 100 mg ground leaves spiked with 1 µg MeSA in positive and negative modes.

Figure 5 presents 2D SPME-MCC-IMS plots of the head space of 100 mg ground leaves spiked with 1 µg MeSA for four different MCCs (OV1, OV5, OV17, and OV20) in the negative and positive modes. These plots show 2D separation of the compounds in MCC (retention time, y-axis) and in IMS (drift time, x-axis). Depending on the MCC type, different retention times were observed for MeSA. Figure S7 shows, that the retention times of MeSA in OV1, OV5, OV17, and OV20 are about 25, 35, 70, and 44 s, respectively. The 2D MCC-IMS spectra in Figure 5 show that in the positive mode, OV1 cannot separate MeSA peak, partial separation is achieved using OV5 and OV20, while with OV17 complete separation is achieved. In the negative mode, OV5, OV17, and OV20 successfully separated MeSA.

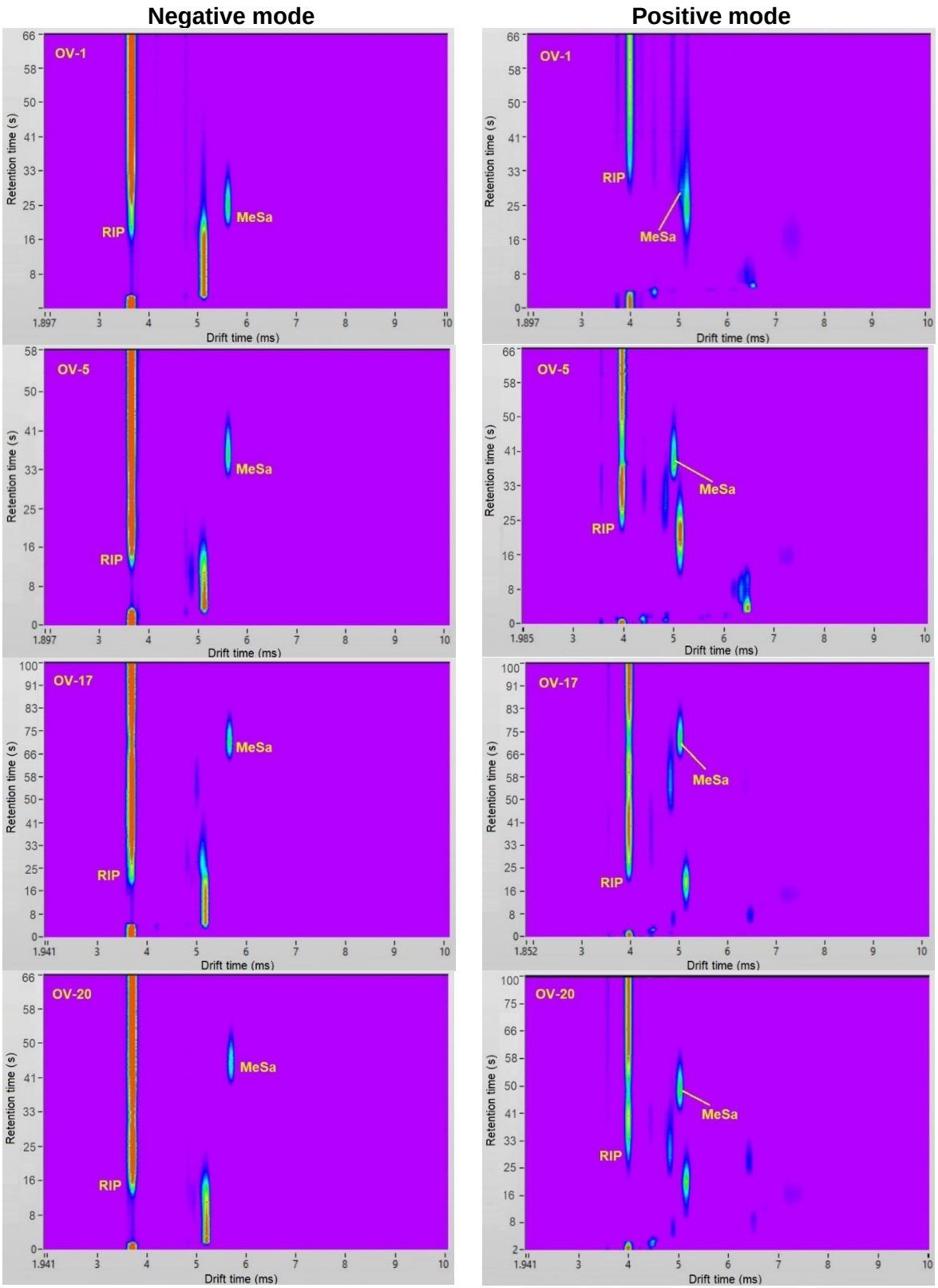

Figure 5. 2D MCC-IMS plots of head space of 100 mg ground leaves obtained by commercial MCC columns OV1, OV5, OV17, and OV20, in the negative and positive modes.

Hence, suitability of a MCC depends to some extent on the IMS polarity. As mentioned above, since in the negative polarity, less matrix interferences appear, the separation is easier in this polarity. As optimal configuration for the quantitative analysis of MeSA in tomato leaves was selected SPME-MCC-IMS method with PDMS fiber, and OV5 column, in the negative IMS polarity.

Two calibration curves were obtained using SPME-MCC-IMS for the standard sample of MeSA and the spiked MeSA in 100 mg ground leaves. The standard and spiked calibration curves are shown in Figure S6 (Supporting information). The obtained LOD and dynamic range for the standard samples were 0.1 μg mL^{-1} and 0.25-14 μg mL^{-1}, respectively. The recovery of the method and relative standard deviation (RSD) for three spiked concentrations 3, 7, and 12 μg g^{-1} were obtained. The results summarized in Table S3 (Supporting information) show that the recoveries are between 92%-107% and the smaller RSDs were obtained for the higher concentrations.

The detection of MeSA in the non-inoculated tomato leaves by GC-MS method, failed.[29,30] In present study a weak MeSA peak was detected for the non-inoculated tomato leaves. This indicates that there is an initial amount of MeSA in tomato leaves before the plant is exposed to ToRSV. This initial amount may be due to an unknown abiotic pathogen in the laboratory. For example, it has been reported that presence of heavy metals such as cadmium in the soil induces releasing of SA and MeSA in plants.[45] The initial amount of MeSA in non-inoculated leaves was determined about be 0.9 μg g^{-1}. After inoculation of the tomato leaves by ToRSV, MeSA was measured from the lower and the upper leaves of the tomato plant (Figure 6a) in 24 h time intervals for four days. Figure 6b shows the SPME-MCC-IMS spectra obtained 48 h after the inoculation. Despite the longer distance from the inoculated leaves, the MeSA content of the upper leaves was higher, compared to the inoculated lower leaves. Figure 6c shows the results of daily measurements of MeSA, 24 to 96 hours after the inoculation. MeSA content reaches its maximum level for both the upper and lower leaves, 48 h after inoculation, then, its amount decreases in accordance with the previous studies.[29] MeSA content 24 h after ToRSV-inoculation was 3 and 2.1 μg g^{-1} in the upper and lower leaves. Although these amounts are low compared to the maximum content, they are substantially larger than in the non-inoculated leaves. The obtained MeSA content of the tomato leaves by SPME-MCC-IMS (1.5-9.8 μg g^{-1}) was slightly higher than those reported previously (1-7 μg g^{-1}).[29,30] During plant growth, some yellow leaves appeared. The SPME-MCC-IMS spectra of a fresh green and a yellow leaf are compared in Figure S8 (Supporting information). In the yellow leaf no MeSA was detected, but also some of the interfering volatile compounds were absent.

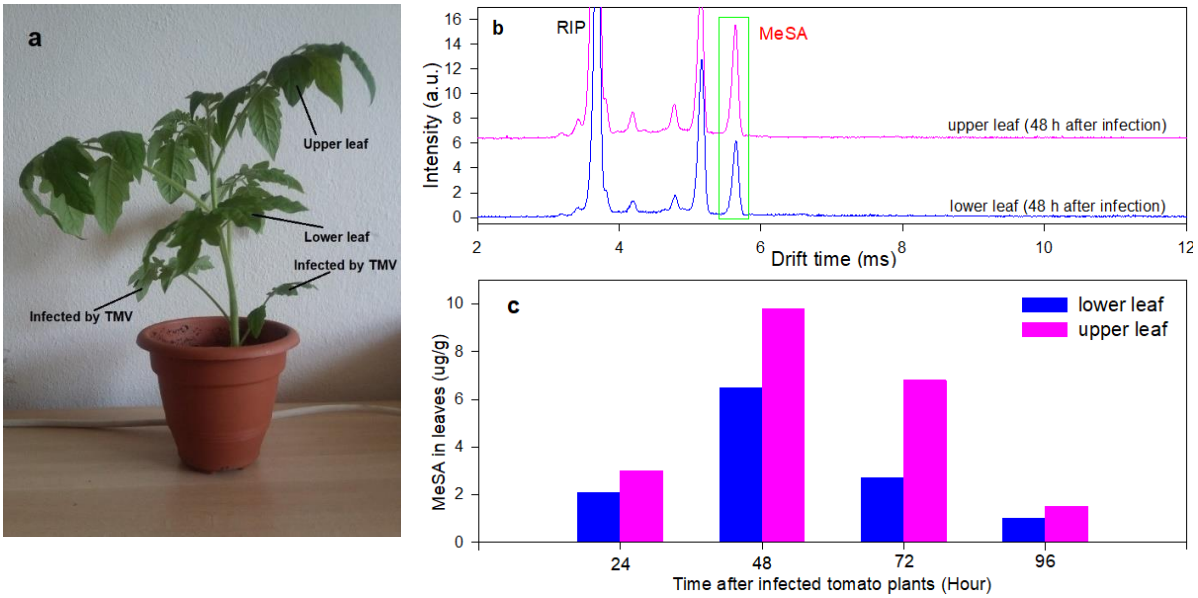

Figure 6. (a) The ToRSV inoculated, lower and upper leaves in a typical tomato plant. (b) The MCC-separated IMS spectra obtained 48 h after inoculation by ToRSV. (c) The measured MeSA content of upper and lower leaves 24 to 96 hours after inoculation.

4. Conclusion

SPME and MCC were coupled to IMS to benefit from their pre-concentration and pre-separation, simultaneously. The SPME-MCC-IMS was applied successfully for the qualitative and quantitative analysis of MeSA in the tomato leaves. The measured MeSA content of the tomato leaves by SPME-MCC-IMS method (1.5-9.8 µg g^{-1}) was in good agreement with those obtained by GC-MS. Using MCC instead of GC column, fast analysis of MeSA content of leaves with a run time of less than 100 s was achieved. Furthermore, MCC-IMS is more affordable than the earlier reported methods for MeSA analysis of the plants. One of the most important advantages of this method is the CD-ion source of IMS which may operate in both positive and negative polarities. By changing the ion source polarity to negative, the interfering matrix molecules were substantially suppressed in the IMS spectra. Finally, optimum combination of SPME fiber materials and MCC column was found for the detection of MeSA by IMS. Present results show, that SPME-MCC-IMS technique is suitable for qualitative and quantitative analysis of volatile compounds released from plants.

Supporting Information

The SPME arrows and their fiber compositions (Table S1); T-shaped setup for measurement of gas sample and calibration curves for gaseous MeSA (Figure S1); Optimized structures of MeSA ions (Figure S2); ΔH and ΔG values for the ionization reaction of MeSA (Table S2); IM spectra of MeSA with and without NH_3 as dopant gas (Figure S3); Effect of extraction temperature on SPME-IMS signal intensity (Figure S4); Comparison of IMS spectra of standard MeSA and head space of tomato leaves for direct analysis without SPME-MCC (Figure S5); Calibration curve with head space SPME method for standard samples and 100 mg tomato leaves spiked with 100 µl MeSA (Figure S6); Retention times of MeSA in different MCCs (Figure S7); The recovery and RSD obtained by SPME-MCC-IMS (Table S3); IM-spectra of green and yellow leaves with SPME-MCC-IMS (Figure S9).

Author Information

Corresponding Authors

Vahideh Ilbeigi, https://orcid.org/0000-0001-9112-8381, conceptualization, methodology, experimental work, data analysis, validation, writing.

Štefan Matejčík, https://orcid.org/0000-0001-7238-5964, supervising, funding acquisition, project administration, writing – review & editing.

Authors

Younes Valadbeigi, https://orcid.org/0000-0002-4189-2987, DFT calculations, writing – review & editing.

Ľudmila Slováková, https://orcid.org/0000-0002-4464-5332, plant treatment, review & editing

Notes

The authors declare no competing financial interest.

Acknowledgments

The research presented in this paper received funding from the European Union's Horizon 2020 research and innovation programme under the Marie Sklodowska-Curie grant agreement No 101031538. The project was partially supported by Slovak Research and Development Agency under project Nr. APVV-19-0386 and financially supported by the Slovak Grant Agency VEGA, project Nr. 1/0489/21. The authors thank Dr. Moravsky Ladislav for technical support.

References

(1) Li, J.; Li, C.; Smith, M. Hormone Metabolism and Signaling in Plants. 1st Ed.; Academic Press, Elsevier Ltd, 2017.
(2) Weyers, J. D. B.; Paterson, N. W. Plant Hormones and the Control of Physiological Processes. *New Phytol*. **2002**, *152*, 375-407.
(3) Weiler, E. W. Plant Hormone Immunoassay. *Physiol. Plant*. **1982**, *54*, 230-234.
(4) Reeve, D. R.; Crozier, A. Quantitative Analysis of Plant Hormones. In: MacMillan, J. ed. Hormonal Regulation of Development I. Molecular aspects of Plant Hormones. pp. 203– 280; Springer-Verlag, Berlin, Germany, 1980.
(5) Davis, P. J. Plant Hormones: Biosynthesis, Signal Transduction, Action. 3rd Ed.; Springer, Dordrecht, 2010.
(6) Zhang, Z.; Huang, Y.; Ding, W.; Li, G. Multilayer Interparticle Linking Hybrid MOF-199 for Noninvasive Enrichment and Analysis of Plant Hormone Ethylene. *Anal. Chem*. **2014**, *86*, 3533−3540.
(7) Wang, M.; Liang, S.; Bai, L.; Qiao, F.; Yan, H. Green Protocol for the Preparation of Hydrophilic Molecularly Imprinted Resin in Water for the Efficient Selective Extraction and Determination of Plant Hormones from Bean Sprouts. *Anal. Chim. Acta* **2019**, *1064*, 47-55.
(8) Yan, H.; Wang, F.; Han, D.; Yang, G. Simultaneous Determination of Four Plant Hormones in Bananas by Molecularly Imprinted Solid-Phase Extraction Coupled with High Performance Liquid Chromatography. *Analyst*, **2012**, *137*, 2884-2890.
(9) Lu, Y.; Li, P.; Yang, C.; Han, Y.; Yan, H. One Pot Green Synthesis of m-Aminophenol–Urea–Glyoxal Resin as Pipette Tip Solid-Phase Extraction Adsorbent for Simultaneous Determination of Four Plant Hormones in Watermelon Juice. *J. Chromatogr. A* **2020**, *1623*, 461214.
(10) Song, X. Y.; Ha, W.; Chen, J.; Shi, Y.P. Application of ß-Cyclodextrin-Modified, Carbon Nanotube-Reinforced Hollow Fiber to Solid-Phase Microextraction of Plant Hormones. *J. Chromatogr. A* **2014**, *1374*, 23-30.
(11) Si, R.; Han, Y.; Wu, D.; Qiao, F.; Bai, L.; Wang, Z.; Yan, H. Ionic Liquid-Organic-Functionalized Ordered Mesoporous Silica-Integrated Dispersive Solid-Phase Extraction for Determination of Plant Growth Regulators in Fresh Panax Ginseng. *Talanta* **2020**, *207*, 120247.
(12) Lisko, J. G.; Stanfill, S. B.; Watson, C. H. Quantitation of Ten Flavor Compounds in Unburned Tobacco Products. *Anal. Methods* **2014**, *6*, 4698-4704.
(13) Niu, Q.; Zong, Y.; Qian, M.; Yang, F.; Teng, Y. Simultaneous Quantitative Determination of Major Plant Hormones in Pear Flowers and Fruit by UPLC/ESI-MS/MS. *Anal. Methods* **2014**,*6*, 1766-1773.
(14) Izumi, Y.; Okazawa, A.; Bamba, T.; Kobayashi, A.; Fukusaki, E. Development of a Method for Comprehensive and Quantitative Analysis of Plant Hormones by Highly Sensitive Nanoflow Liquid Chromatography–Electrospray Ionization-Ion Trap Mass Spectrometry. *Anal. Chim. Acta* **2009**, *648*, 215-225.
(15) Durgbanshi, A.; Arbona, V.; Pozo, O.; Miersch, O.; Sancho, J. V.; Gómez-Cadenas, A. Simultaneous Determination of Multiple Phytohormones in Plant Extracts by Liquid Chromatography−Electrospray Tandem Mass Spectrometry. *J. Agric. Food Chem.* **2005**, *53, 22*, 8437–8442.
(16) Bosco, R.; Daeseleire, E.; Pamel, E. V.; Scariot, V.; Leus, L. Development of An Ultrahigh-Performance Liquid Chromatography− Electrospray Ionization−Tandem Mass Spectrometry Method for the Simultaneous Determination of Salicylic Acid, Jasmonic Acid, and Abscisic Acid in Rose Leaves. *J. Agric. Food Chem*. **2014**, *62*, 6278−6284.

(17) Wang, Q.; Cai, W. J.; Yu, L.; Ding, J.; Feng, Y. Q. Comprehensive Profiling of Phytohormones in Honey by Sequential Liquid−Liquid Extraction Coupled with Liquid Chromatography− Mass Spectrometry. *J. Agric. Food Chem*. **2017**, *65*, 575−585.
(18) Liu, B. F.; Zhong, X. H.; Lu, Y. T. Analysis of Plant Hormones in Tobacco Flowers by Micellar Electrokinetic Capillary Chromatography Coupled with On-Line Large Volume Sample Stacking. *J. Chromatogr. A* **2002**, *945*, 257-265.
(19) Carretero, A. S.; Cruces-Blanco, C.; Peña, M. S.; Ramírez, S. C.; Gutiérrez, A. F. Determination of Phytohormones of Environmental Impact by Capillary Zone Electrophoresis. *J. Agric. Food Chem*. **2004**, *52*, 1419–1422.
(20) Wang, F.; Gu, X.; Zheng, C.; Dong, F.; Zhang, L.; Cai, Y.; You, Z.; You, J.; Du, S.; Zhang, Z. Ehrlich Reaction Evoked Multiple Spectral Resonances and Gold Nanoparticle Hotspots for Raman Detection of Plant Hormone. *Anal. Chem*. **2017**, *89*, 8836−8843.
(21) Naqvi, S. M. Z. A.; Zhang, Y.; Ahmed, S.; Abdulraheem, M. I.; Hu, J.; Tahir, M. N.; Raghavan, V. Applied Surface Enhanced Raman Spectroscopy in Plant Hormones Detection, Annexation of Advanced Technologies: A review. *Talanta* **2022**, *236*, 122823.
(22) Zhang, C.; Žukauskaitė, A.; Petřík, I.; Pěnčík, A.; Hönig, M.; Grúz, J.; Široká, J.; Novák, O.; Doležal, K. In Situ Characterisation of Phytohormones from Wounded Arabidopsis Leaves Using Desorption Electrospray Ionisation Mass Spectrometry Imaging. *Analyst*, **2021**,*146*, 2653-2663.
(23) Shulaev, V.; Silverman, P.; Raskin, l. Airborne Signalling by Methyl Salicylate in Plant Pathogen Resistance. *Nature* **1997**, *385*, 718-721.
(24) Parker, D.; Martinez, C.; Stanley, C.; Simmons, J.; Mclntyre, l. M. The Analysis of Methyl Salicylate and Salicylic Acid from Chinese Herbal Medicine Ingestion. *J. Anal. Toxicol*. **2004**, *28*, 214-216.
(25) Chen, C.; Yang, L. L.; Tang, A. L.; Wang, P. Y.; Dong, R.; Wu, Z. B.; Li, Z.; Yang, S. Curcumin−Cu(II) Ensemble-Based Fluorescence “Turn-On” Mode Sensing the Plant Defensive Hormone Salicylic Acid In Situ and In Vivo. *J. Agric. Food Chem*. **2020**, *68*, 4844−4850.
(26) Huang, J.; Cardoza, Y. J.; Schmelz, E. A.; Raina, R.; Engelberth, J.; Tumlinson, J. H. Differential Volatile Emissions and Salicylic Acid Levels from Tobacco Plants in Response to Different Strains of Pseudomonas Syringae. *Planta* **2003**, *217*, 767–775.
(27) Patel, S. V.; Hobson, S. T.; Cemalovic, S.; Mlsna, T. E. Detection of Methyl Salicylate Using Polymer-Filled Chemicapacitors. *Talanta* **2008**, *76*, 872-877.
(28) Umasankar, Y.; Ramasamy, R. P. Highly Sensitive Electrochemical Detection of Methyl Salicylate Using Electroactive Gold Nanoparticles. *Analyst*, **2013**, *138*, 6623-6631.
(29) Deng, C.; Qian, J.; Zhu, W.; Yang, X.; Zhang, X. Rapid Determination of Methyl Salicylate, A Plant-Signaling Compound, in Tomato Leaves by Direct Sample Introduction and Thermal Desorption Followed by GC-MS. *J. Sep. Sci.* **2005**, *28*, 1137-1142.
(30) Deng, C.; Zhang, X.; Zhu, W.; Qian, J. Gas Chromatography-Mass Spectrometry with Solid-Phase microextraction method for determination of methyl salicylate and other volatile compounds in leaves of Lycopersicon Esculentum. *Anal. Bioanal. Chem*. **2004**, *378*, 518–522.
(31) Deng, W. W.; Wang, R.; Yang, T.; Jiang, L.; Zhang, Z. Z. Functional Characterization of Salicylic Acid Carboxyl Methyltransferase from Camellia sinensis, Providing the Aroma Compound of Methyl Salicylate during the Withering Process of White Tea. *J. Agric. Food Chem*. **2017**, *65*, 11036−11045.
(32) Eiceman, G. A.; Karpas, Z.; Hill, Jr, H.H. Ion Mobility Spectrometry. 3rd Ed. CRC Press, Taylor & Francis Group, Boca Raton, Fl, 2014.
(33) Sabo, M.; Matejcik, S. A Corona Discharge Atmospheric Pressure Chemical Ionization Source with Selective NO^+ Formation and Its Application for Monoaromatic VOC Detection. *Analyst* **2013**, *138*, 6907-6912.
(34) Tabrizchi, M.; Ilbeigi, V. Detection of Explosives by Positive Corona Discharge Ion Mobility Spectrometry. *J. Hazard. Mater*. **2010**, *176*, 692-696.
(35) Borsdorf, H.; Eiceman, G. A. Ion Mobility Spectrometry: Principles and Applications, *Appl.Spec. rev.***2006**, *41*, 323-375.
(36) Waraksa, E.; Perycz, U.; Namiesnik, J.; Sillanpaa, M.; Dymerski, T.; Wojtowicz, M.; Puton, J. Dopants and Gas Modifiers in Ion Mobility Spectrometry. *Trend Anal. Chem*. **2016**, *82*, 237-249.
(37) Marchand, A.; Livet, S.; RosU, F.; Gabelica, V. Drift Tube Ion Mobility: How to Reconstruct Collision Cross Section Distributions from Arrival Time Distributions? *Anal. Chem*. **2017**, *89*, 12674–12681.
(38) Guerra, P.; Lai, H.; Almirall, J. R. Analysis of the Volatile Chemical Markers of Explosives Using Novel Solid Phase Microextraction Coupled to Ion Mobility Spectrometry. *J. Sep. Sci*. **2008**, *31*, 2891-2898.

(39) Jafari, M. T.; Saraji, M.; Ameri, A. H. Coupling of Solid Phase Microextraction with Electrospray Ionization Ion Mobility Spectrometry and Direct Analysis of Venlafaxine in Human Urine and Plasma. *Anal. Chim. Acta* **2015**, *853*, 460-468.
(40) Wolf, A.; Baumbach, J. I.; Kleber, A.; Maurer, F.; Maddula, S.; Favrod, P.; Jang, M.; Fink, T.; Volk, T.; Kreuer, S. Multi-Capillary Column-Ion Mobility Spectrometer (MCC-IMS) Breath Analysis in Ventilated Rats: A Model with the Feasibility of Long-Term Measurements. *J. Breath Res.* **2014**, *8*, 016006.
(41) Sihelská, N.; Vozárová, Z.; Predajňa, L.; Šoltys, K.; Hudcovicová, M.; Mihálik, D.; Kraic, J.; Mrkvová, M.; Kúdela, O.; Glasa, M. Experimental Infection of Different Tomato Genotypes with Tomato mosaic virus Led to a Low Viral Population Heterogeneity in the Capsid Protein Encoding Region. *Plant Pathol. J.* **2017**, *33*, 508-513.
(42) Gaussian 16, Revision C.01, Frisch, M. J.; Trucks, G. W.; Schlegel, H. B.; Scuseria, G. E.; Robb, M. A.; Cheeseman, J. R.; Scalmani, G.; Barone, V.; Petersson, G. A.; Nakatsuji, H.; Li, X.; Caricato, M.; Marenich, A. V.; Bloino, J.; Janesko, B. G.; Gomperts, R.; Mennucci, B.; Hratchian, H. P.; Ortiz, J. V.; Izmaylov, A. F.; Sonnenberg, J. L.; Williams-Young, D.; Ding, F.; Lipparini, F.; Egidi, F.; Goings, J.; Peng, B.; Petrone, A.; Henderson, T.; Ranasinghe, D.; Zakrzewski, V. G.; Gao, J.; Rega, N.; Zheng, G.; Liang, W.; Hada, M.; Ehara, M.; Toyota, K.; Fukuda, R.; Hasegawa, J.; Ishida, M.; Nakajima, T.; Honda, Y.; Kitao, O.; Nakai, H.; Vreven, T.; Throssell, K.; Montgomery, J. A., Jr.; Peralta, J. E.; Ogliaro, F.; Bearpark, M. J.; Heyd, J. J.; Brothers, E. N.; Kudin, K. N.; Staroverov, V. N.; Keith, T. A.; Kobayashi, R.; Normand, J.; Raghavachari, K.; Rendell, A. P.; Burant, J. C.; Iyengar, S. S.; Tomasi, J.; Cossi, M.; Millam, J. M.; Klene, M.; Adamo, C.; Cammi, R.; Ochterski, J. W.; Martin, R. L.; Morokuma, K.; Farkas, O.; Foresman, J. B.; Fox, D. J. Gaussian, Inc., Wallingford CT, 2016.
(43) Fanga, Y.; Bullockb, H.; Leec, S. A.; Sekara, N.; Eitemanc, M. A.; Whitmanb, W. B.; Ramasamya, R. P. Detection of Methyl Salicylate Using Bi-Enzyme Electrochemical Sensor Consisting Salicylate. *Biosens. Bioelectron*. **2016**, *85*, 603-610.
(44) Chen, Y.; Fegadolli, W. S.; Jones, W. M.; Scherer, A.; Li, M. Ultrasensitive Gas-Phase Chemical Sensing Based on Functionalized Photonic Crystal Nanobeam Cavities. *ACS Nano*, **2014**, *8*, 522–527.
(45) Guo, B.; Liu, C.; Liang, Y.; Li, N.; Fu, Q. Salicylic Acid Signals Plant Defence against Cadmium Toxicity. *Int. J. Mol. Sci*. **2019**, *20*, 2960.

Solid Phase Microextraction-Multi Capillary Column-Ion Mobility Spectrometry (SPME-MCC-IMS) for Detection of Methyl Salicylate in Tomato Leaves

Vahideh Ilbeigi[1], Younes Valadbeigi[2,3], Ľudmila Slováková[4] and Štefan Matejčík[1]

[1]Department of Experimental Physics, Comenius University, Mlynská dolina F2, 84248 Bratislava, Slovakia

[2] Department of Chemistry, Faculty of Science, Imam Khomeini International University, Qazvin, Iran.

[3] University of Natural Resources and Life Sciences, Department of Chemistry, Institute of Analytical Chemistry, 1190 Vienna, Austria

[4] Department of Plant Physiology, Faculty of Natural Sciences, Mlynská dolina, Ilkovičova 6, 842 15 Bratislava 4, Slovakia

Emails: vahideh.ilbeigi@fmph.uniba.sk; stefan.matejcik@fmph.uniba.sk

Table of content